frontiers | Frontiers in Physics

TYPE Original Research
PUBLISHED 06 February 2024
DOI 10.3389/fphy.2024.1312930

OPEN ACCESS

EDITED BY
Huan Yang,
Shandong University, China

REVIEWED BY
Jinhui Wu,
Northeast Normal University, China
Bao-Sen Shi,
University of Science and Technology of China, China

*CORRESPONDENCE
Jun He,
hejun@sxu.edu.cn
Renfu Yang,
yangrf@baqis.ac.cn

RECEIVED 10 October 2023
ACCEPTED 25 January 2024
PUBLISHED 06 February 2024

CITATION
Du Y, Cong N, Liu Y, Lyu Z, He J and Yang R (2024), Enhanced microwave-atom coupling via quadrupole transition-dressed Rydberg atoms.
Front. Phys. 12:1312930.
doi: 10.3389/fphy.2024.1312930

Enhanced microwave-atom coupling via quadrupole transition-dressed Rydberg atoms

Yijie Du[1,2], Nan Cong[1], Yao Liu[3], Ziyao Lyu[2], Jun He[3]* and Renfu Yang[1]*

[1]Beijing Academy of Quantum Information Sciences, Beijing, China, [2]State Key Laboratory of Space Ground Integrated Information Technology, and Beijing Institute of Satellite Information Engineering, Beijing, China, [3]State Key Laboratory of Quantum Optics and Quantum Optics Devices, Institute of Opto-Electronics, and Collaborative Innovation Center of Extreme Optics, Shanxi University, Taiyuan, China

The power broadening of a coupling laser can be converted into two-photon detuning by electromagnetically induced transparency (EIT), resulting in a residual Doppler effect. The residual Doppler effect in a ladder-type EIT in a room-temperature atom ensemble is further amplified through a wavelength mismatch effect between the probe and coupling laser beams, which reduces the atomic coupling of light or microwaves. We measured the Rydberg spectra of the electric dipole (E1) and electric quadrupole (E2) microwave transitions, demonstrating that the reduction in the Rydberg EIT signal can be recovered through far-off-resonance E2 microwave transition dressing and achieving an 8-dB enhancement in the Rydberg EIT signal. The frequency-dependent dressing of the E2 transition enables the shift of the dressed Rydberg states to be tuned, thereby providing a scalable approach to optimize the interaction between the Rydberg state and microwave field.

KEYWORDS

Rydberg atoms, microwave measurement, electromagnetically induced transparency, quadrupole transition, electric field

1 Introduction

Rydberg atoms are promising candidates for microwave (MW) electric field measurements owing to their high polarizability and strong electric dipole moments [1–9]. In a room-temperature atomic ensemble of Cs atoms, the inhomogeneous broadening of Doppler effect σ (~350 MHz) is larger than the homogeneous broadening of the spontaneous decay linewidth Γ of the 6P state (~5.2 MHz). The current experimental study suppresses the velocity-dependent inhomogeneous spectral broadening in precise Rydberg spectroscopy via Doppler-free configurations. Electromagnetically induced transparency (EIT) is a destructive interference effect with a narrow linewidth. Sub-Doppler Rydberg EIT spectroscopy can be achieved using two-photon excitation. The power broadening of a coupling laser with a ladder-type EIT in a room-temperature ensemble can be converted into two-photon detuning or broadening [10–13]. This residual Doppler effect is further amplified as the wave vector mismatch between the probe and the coupling laser, which reduces the atomic absorption [14–16].

Recent studies on atomic clocks and interferometry have counteracted inhomogeneous broadening or shift using a magic or tune-out wavelength [17–19]. In these scenarios, multiple-field dressings allow the atomic degrees of freedom to be tuned and thereby improve coupling. More recent studies have used MW-dressed Rydberg atoms to tune

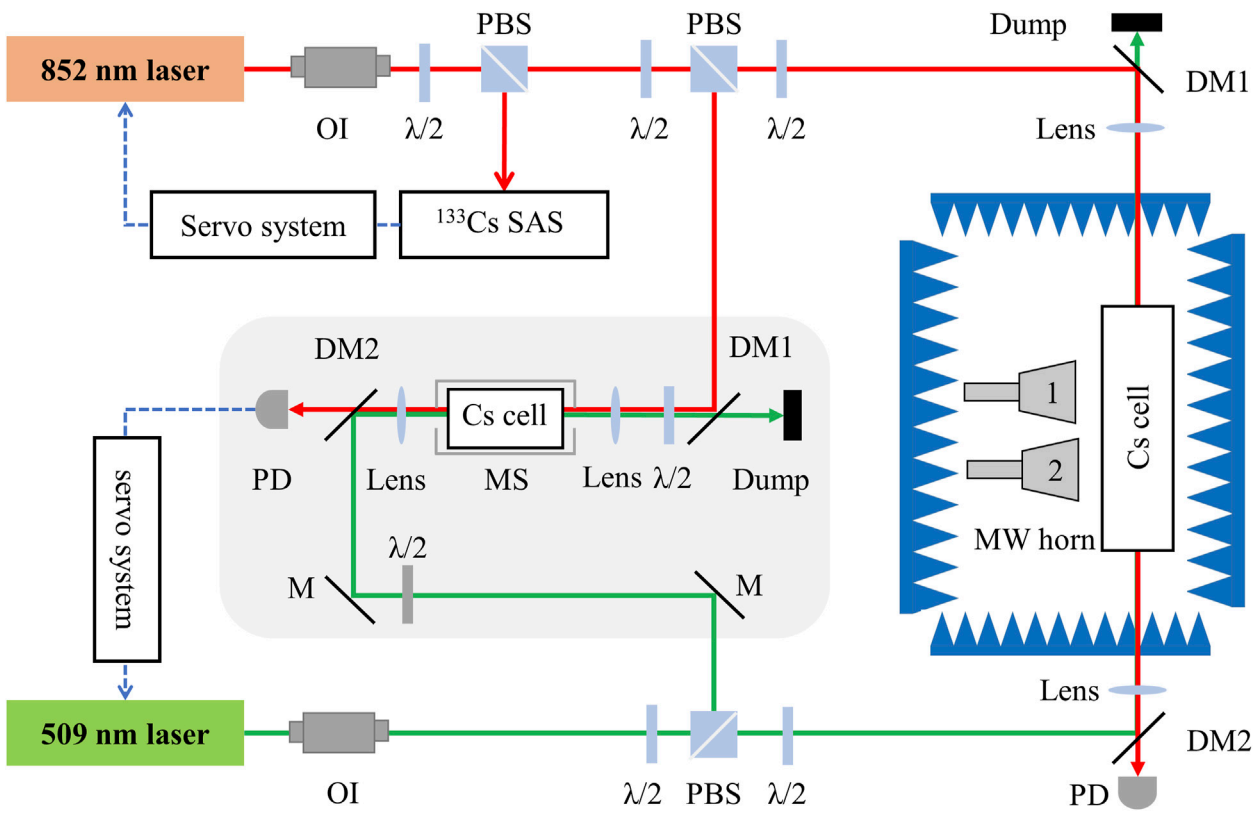

FIGURE 1
Schematic of the experimental apparatus. Using a counterpropagating configuration, the probe and coupling beams (wavelengths 852 nm and 509 nm, respectively) overlap in the Cs atomic vapor cell. The frequency of the probe beam is stabilized to the hyperfine transition via saturation absorption spectroscopy (SAS). The frequency of the coupling beam is stabilized in the Cs-cell through Rydberg atom EIT spectroscopy. OI: optical isolator; λ/2: half-wave plate; PBS: polarizing beam splitter cube; MS: magnetic shielding; PD: photodiode detector; DM1: 852-nm high-reflectivity (HR) and 509-nm high-transmissivity (HT) dichroic mirror; DM2: 852-nm HT and 509 nm HR dichroic mirror; Dump: optical dump.

atom–atom interactions [20–22]. These approaches have can also suppress spectral broadening or atomic decoherence [19, 23–26]; however, resonance transition dressings cause undesired Rydberg-state populations and introduce additional broadening. In contrast, far-off-resonance MW dressing offers an effective shift in the state but is less effective in modifying dressing polarization owing to its frequency insensitivity.

In this study, an auxiliary field dressing for the electric quadrupole (E2) transition is used to counteract inhomogeneous spectral broadening. The reduction in atomic coupling of the optical and MW fields can be recovered by E2 transition dressing. The E2 transition modifies both the dressing shift and polarization. The dressing developed in this study provides a new method for recovering velocity-dependent residual Doppler effects in ladder-type EIT.

2 Experimental methods

The experimental apparatus (Figure 1) includes an external cavity diode laser operating at a wavelength of 852 nm to generate a probe beam and a fiber laser operating at a wavelength of 509 nm to produce a coupling laser beam. Their linewidths are approximately 100 kHz and 20 kHz, respectively. The probe laser frequency was stabilized to the Cs D_2 transition $6S_{1/2}$ (F = 4) → $6P_{3/2}$ (F = 5) via saturation absorption spectroscopy (SAS). The frequency of the coupling laser beam was stabilized by Rydberg atom EIT spectroscopy. A cylindrical cell with a length and diameter of 75 mm and 25 mm, respectively, confines the Cs vapor at room temperature. The MW field was transmitted to the vapor cell through a standard gain horn antenna, and the MW signal generator (Rohde & Schwarz, SMA100B) was stabilized using a Rb atomic clock (Stanford Research Systems, FS725). The probe laser power used in the experiment is 20 μW, and the diameter is 0.65 mm. The corresponding Rabi frequency is and $\Omega_p = 2\pi \times 4.98$ MHz. The coupling laser power used in the experiment is 80 mW, and the diameter is 0.85 mm the corresponding Rabi frequency is and $\Omega_c = 2\pi \times 0.4$ MHz. The atomic density is 5.97×10^{10} cm^{-3}. The probe laser beam was recorded using a photodiode detector (PD), and an oscilloscope (Keysight, DSOX3024T) and a spectrum analyzer (Keysight, 9030 B) were used to record and process the transmitted signal.

The transition spectra of the MW frequency-related E1 and E2 transitions [Figure 2B] were measured by probing the EIT signals using an amplitude modulation (AM) technique for EIT signals. The dipole moments of the two microwave transitions are 5,445 a_0e ($72\ S_{1/2} \rightarrow 72\ P_{1/2}$) and 5,240 a_0e ($72\ S_{1/2} \rightarrow 72\ P_{3/2}$), respectively. The quadrupole moments of the two microwave transitions are 2.334×10^{-3} a_0e ($72\ S_{1/2} \rightarrow 70\ D_{3/2}$) and 2.352×10^{-3} a_0e ($72\ S_{1/2} \rightarrow 70\ D_{5/2}$), respectively. In this experiment, 100% AM at 131 kHz was

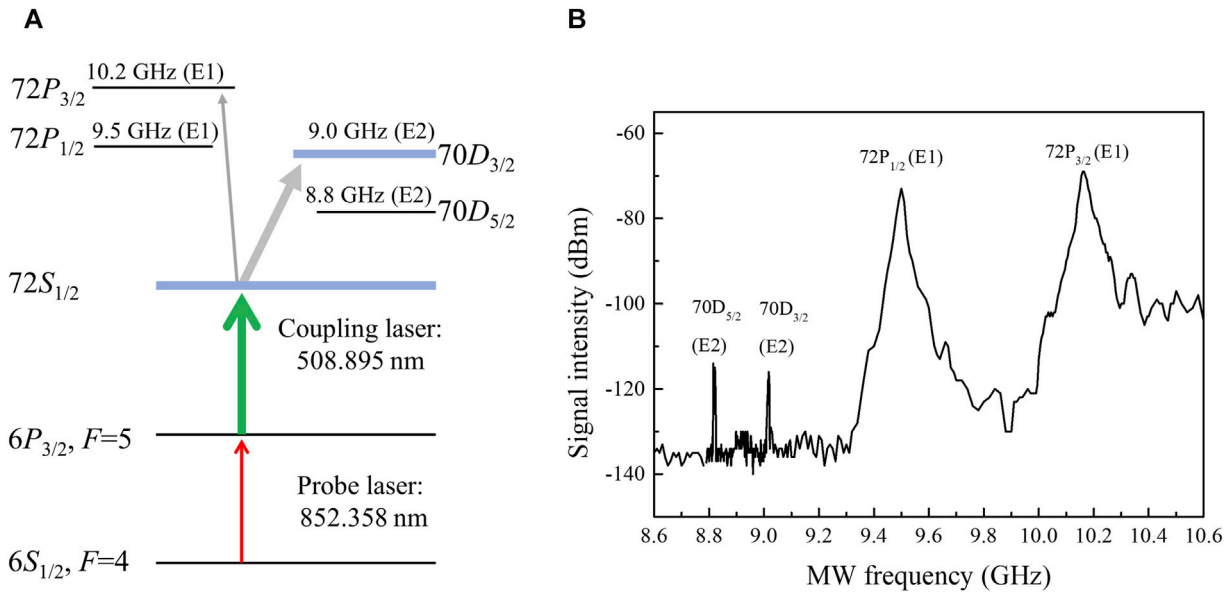

FIGURE 2
(A) Atomic energy level diagram of Cs associated with Rydberg EIT signals. **(B)** Spectral characterization of the dipole (E1) and quadrupole (E2) transitions. The EIT signal intensity is measured by AM probing. The MW field transmission power level is fixed while the MW frequency is scanned from 8.6 to 10.6 GHz in steps of 2 MHz. The probe and coupling lasers are frequency stabilized to the $6S_{1/2}\rightarrow6P_{3/2}\rightarrow72S_{1/2}$ transitions through EIT spectroscopy. The Rabi frequencies of the probe and coupling beams are $2\pi \times 4.98$ MHz and $2\pi \times 0.4$ MHz, respectively.

applied to the signal and demodulated using a spectrum analyzer with a resolution bandwidth of 1 Hz. The MW frequency was scanned from 8.6 to 10.6 GHz in steps of 2 MHz.

3 Results and discussion

The coupled atomic energy levels of Cs participating in ladder-type EIT (Figure 2A) involve two optical fields of wavelengths 852 nm and 509 nm corresponding to $6S_{1/2}\rightarrow6P_{3/2}$ and $6P_{3/2}\rightarrow72S_{1/2}$ transitions, respectively. The E1 transitions couple the $72S_{1/2}$ states to the $72P_{1/2}$ and $72P_{3/2}$ states with corresponding MW transition frequencies of 9.50 GHz and 10.17 GHz, respectively. Similarly, the E2 transitions couple the $72S_{1/2}$ state to the $70D_{5/2}$ and $70D_{3/2}$ states with corresponding transition frequencies of 8.82 GHz and 9.02 GHz, respectively. The E2 transition is of the order a_0^2, where a_0 is the Bohr radius; thus, the E2 transition is always three to four orders of magnitude smaller than a typical E1 transition. The transition spectra of the MW frequency-related E1 and E2 transitions (Figure 2B) were measured by probing the EIT signals using an amplitude modulation (AM) technique for EIT signals.

The measured peaks are consistent with the resonance transition characteristics of both the E1 and E2 transitions. The signal intensity of the E2 transition at 8.82 GHz ($72S_{1/2}\rightarrow70D_{5/2}$) is approximately 42 dB weaker than that of the E1 transition at 9.50 GHz ($72S_{1/2}\rightarrow72P_{1/2}$). To investigate the differences in the performance between the frequency-related E1 and E2 transitions, the full width at half maximum (FWHM) of these transitions were measured. The FWHM of both E2 transitions at 8.82 GHz ($72S_{1/2}\rightarrow70D_{5/2}$) and 9.02 GHz ($72S_{1/2}\rightarrow70D_{3/2}$) is ~10 MHz. In contrast, the FWHM of both E1 transitions at 9.50 GHz ($72S_{1/2}\rightarrow72P_{1/2}$) and 10.17 GHz ($72S_{1/2}\rightarrow72P_{3/2}$) is significantly higher at ~200 MHz. The broadening mechanism for E1 transitions primarily involves an inhomogeneous broadening of wavelength mismatch from the excitation laser beams, that is, $\sigma_R = (\lambda_p/\lambda_c)\Gamma_{6P}$, and Stark shifts induced by the off-resonant MW field, that is, $\sigma_S = \sqrt{\Omega^2 + \Delta^2}$, where Δ is the off-resonant detuning.

To further explore the frequency shifts of the Rydberg E1 and E2 transitions, the shifts were recorded at different MW emission powers. With a sufficiently strong interaction in the $72S_{1/2}\rightarrow72P_{3/2}$ transition, Autler–Townes splitting of the Rydberg E1 signal occurs (Figure 3A). The shapes of the EIT-AT peaks are asymmetric at a high-level radio frequency (RF) transmitted strength primarily owing to the inhomogeneous distribution of the space RF field over the vapor cell, but also partly due to the small amount of ionization [27, 28]. When the intermediate-level detuning of the E2 transition is larger than the width of the E1 transition, the E2 interaction can be considered an AC Stark effect through off-resonance excitation. The magnitude of the power-dependent shift of the E2 transition increases with the MW field power (Figure 3B). The spectral linewidth increases from ~1 to 80 MHz as the MW power increases from −30 dBm to 20 dBm. Shift measurements are shown in the inset of Figure 3B.

A sub-Doppler spectrum of the $6S_{1/2}\rightarrow6P_{3/2}\rightarrow72S_{1/2}$ Rydberg EIT signal was obtained using counterpropagating excitation beams from the probe and coupling lasers. The typical EIT linewidth measures several tens of megahertz [7, 12, 28, 29], which is considerably larger than the spontaneous emission linewidth of Rydberg states. These spectral broadenings include spontaneous emission broadening of the intermediate levels and power broadening of the coupling laser beam, the latter of which can be converted into two-photon detuning using the EIT scheme, resulting in a velocity-dependent residual Doppler effect. The residual Doppler effect in the ladder-type EIT of the Rydberg atom may be amplified through a wavelength mismatch associated with a larger wavelength difference between the probe and coupling laser

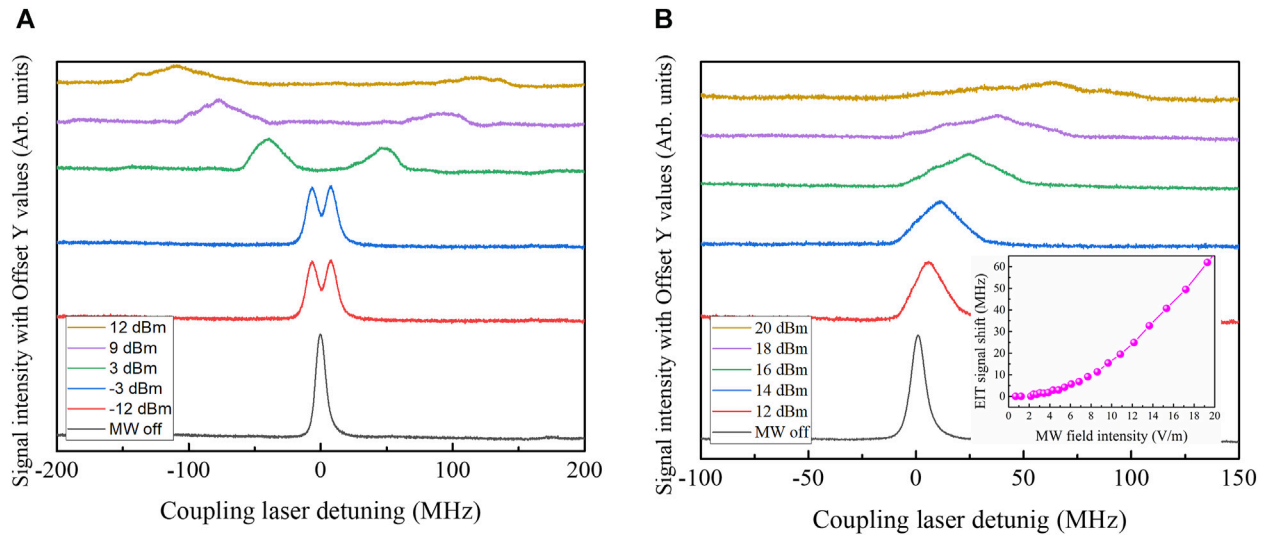

FIGURE 3
Shifts in E1 and E2 transition responses as a function of MW power: **(A)** Autler–Townes splitting induced by the E1 resonance transition; **(B)** shift in E2 transition induced by the AC Stark effect. Spectral broadenings caused by power-dependent resonant coupling. Inset: shifts in the E2 signal as a function of MW power.

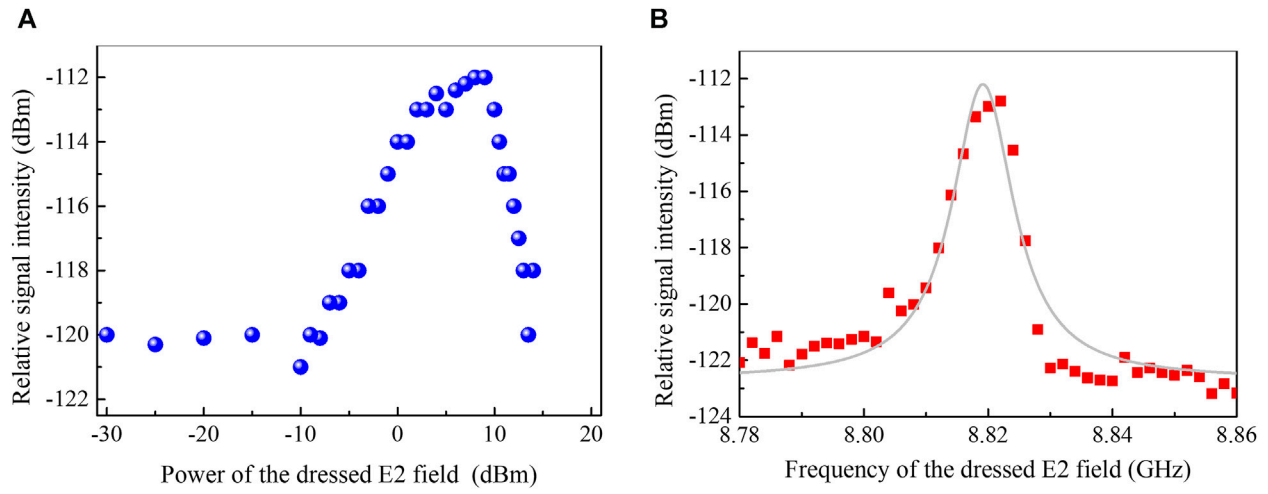

FIGURE 4
Enhanced E1 coupling via E2 transition-dressed Rydberg atoms: **(A)** Signal response of the 9.50-GHz E1 transition as a function of the auxiliary field. The signal magnitude is not affected by an E2 field with a power of less than −10 dBm but quickly increases as the power increases from −10 to 10 dBm. **(B)** Dependence of the signal magnitude on the frequency of the auxiliary field. A Voigt fit (gray curve) of the data yields a linewidth of approximately 10.5 MHz for a typical E2 transition.

beams. The linewidth of the $6P_{3/2}$ intermediate state is Γ_{6p} = 5.2 MHz, which yields a fundamental spectral wavelength mismatch limit of $\sigma_R = (\lambda_p/\lambda_c)\Gamma_{6p}$ = 8.7 MHz. Inhomogeneous broadening of the residual Doppler effect, which scales as Γ/σ, may reduce atomic coupling of the MW fields.

An auxiliary dressing of the E2 transition was employed to recover the atomic E1 transition coupling of the MW field, thereby alleviating the inhomogeneous broadening of the residual Doppler effect and enhancing the atomic coupling of the MW field. The E1 transition of $72S_{1/2}\rightarrow72P_{1/2}$ and the E2 transition of $72S_{1/2}\rightarrow72D_{5/2}$ were chosen as the signal MW field and dressing field, respectively. These 2 MW fields were transmitted to the vapor cell via two standard horn gain antennas. A previous study has derived the compensation condition $\Omega_c^2/(\Delta_c - \delta_c) = \Omega_a^2/(\Delta_a - \delta_a)$ for absorption loss due to Doppler mismatch; here, Ω is the Rabi frequency, Δ is the frequency detuning, and δ is the frequency shift. The subscripts "c" denotes the coupling laser, and "a" denotes the auxiliary or dressing field [16]. The E1 transition was fully recovered to the homogeneous absorption level in an inhomogeneous broadening atomic ensemble during an experimental demonstration [16]; therefore, we hypothesize that the MW coupling of the Rydberg E1 transition, $72S_{1/2}\rightarrow72P_{1/2}$, may

be enhanced by tailoring the effective linewidth of the Rydberg state to satisfy the aforementioned compensation condition. We monitored the AM probe signal using an EIT apparatus. Figure 4A shows the magnitude dependence of the E1 signal field on the power of the E2 dressed field. As the magnitude of E2 field increases from −10 to 10 dBm, the AM probe signal magnitude rapidly increases; the $72S_{1/2}$ state is modulated through the E2 dressing field, and the inhomogeneous broadening of the $72S_{1/2}$ state is compensated. Compensation of the inhomogeneity broadening can recover the fraction of the atomic absorption cross section and enhance microwave coupling. In particular, the signal magnitude reaches a maximum when the power of the E2 field is 10 dBm. Under these conditions, the absorption cross sections of the $72P_{1/2}$ and $72S_{1/2}$ states are substantially recovered. With a further increase in power, the AM signal magnitude decreases because the E2 dressing broadening of $72S_{1/2}$ is greater than the power broadening of the coupling laser, which increases the inhomogeneous spectral broadening. Under the optimized conditions, the Rabi frequencies of the probe and coupling laser beams are $\Omega_p = 2\pi \times 4.98$ MHz and $\Omega_c = 2\pi \times 0.4$ MHz, respectively. The E2 dressing parameters yields a maximum enhancement factor of approximately 8 dB. The noise limit of the spectrum analyzer is −135 dBm, and the PD electric noise is approximately −130 dBm. Technical noise of ~5 dB results from fluctuations in the laser beam power.

In contrast to the far-off-resonance MW or DC electric field dressing, the shift in the E2 transition dressing is frequency-dependent and therefore has the ability to manipulate the coupling of the Rydberg states. Figure 4B illustrates the dependence of the AM signal magnitude on the E2 transition frequency. This effect was evaluated using a Voigt fit of the data, which provided a linewidth of approximately 10.5 MHz for a typical E2 transition, comparable to those obtained in previous studies [30, 31]. Similarly, the E2 transition of $72S_{1/2} \rightarrow 70D_{3/2}$, which has a resonance frequency of 9.02 GHz, exhibits enhanced coupling and frequency dependence similar to those of the $72S_{1/2} \rightarrow 70D_{5/2}$ transition.

In principle, auxiliary field dressings can recover the coupling near the homogeneous or spontaneous decay limits in a room-temperature atom ensemble; however, in practice, Rydberg atoms are susceptible to excitation and stray environmental electromagnetic fields. Blackbody radiation can couple adjacent Rydberg states in atom ensembles at room temperature, thereby causing energy shifts or mixing [12, 32]. Moreover, optical pumping and polarization introduce polarization broadening of the magnetic quantum number m, which describes vector and tensor polarizabilities [33, 34]. The E2 transition dressing can recover the power-broadening-dependent Doppler effect caused by the coupling laser; however, it is less effective for the factors noted above, which may limit further enhancement of the MW-atom coupling.

4 Conclusion

We report E1 and E2 MW transitions in Rydberg atomic ensembles. The frequency-dependent dressing of E2 transitions allows the shift of Rydberg states to be tuned, thereby offering a scalable approach to optimize the coupling of the MW field by the Rydberg state.

MW dressings are advantageous owing to their practicality. First, using optical dressing, the phase fluctuation of the light fields can be converted into amplitude fluctuations by coupling and dispersion under the EIT scheme. This conversion is sensitive to two-photon detuning. Under conditions of very slow phase fluctuations, the atomic state follows the phase fluctuation, thereby changing the absorption cross-section. The phase fluctuation in the MW field is too small to affect the atomic absorption cross section. This presents a potential advantage over the use of optical dressings. Second, unlike far-off-resonance MW or DC electric field dressings, E2 transition dressings exhibit a frequency-dependent shift, allowing the direction of the shifts of the coupled states to be tuned (Figure 4B). Moreover, the vector and tensor polarizabilities of the E2 transitions in the nS Rydberg state are weak. The higher-order polarizabilities under linearly polarized fields depend only on the absolute value of the magnetic quantum number m. In accordance with the transition selection rules, the magnetic sensitivity of the MW-dressed process may be further inhibited and may substantially suppress field broadening. Considering these factors, the approach described herein has a significant advantage.

Data availability statement

The original contributions presented in the study are included in the article/Supplementary material, further inquiries can be directed to the corresponding authors.

Author contributions

YD: Conceptualization, Investigation, Writing–original draft, Writing–review and editing. NC: Conceptualization, Writing–review and editing, Investigation, Writing–original draft. YL: Writing–original draft, Investigation. ZL: Writing–original draft, Investigation. JH: Conceptualization, Funding acquisition, Supervision, Writing–review and editing, Investigation, Writing–original draft. RY: Conceptualization, Funding acquisition, Investigation, Supervision, Writing–review and editing, Writing–original draft.

Funding

The author(s) declare financial support was received for the research, authorship, and/or publication of this article. This study was supported by the National Natural Science Foundation of China (Grant No. 61875111).

Conflict of interest

The authors declare that the research was conducted in the absence of any commercial or financial relationships that could be construed as a potential conflict of interest.

Publisher's note

References

1. Liu B, Zhang LH, Liu ZK, Zhang ZY, Zhu ZH, Gao W, et al. Highly sensitive measurement of a megahertz rf electric field with a rydberg-atom sensor. *Phys Rev Appl* (2022) 18(1):014045. doi:10.1103/PhysRevApplied.18.014045

2. Yao J, An Q, Zhou Y, Yang K, Wu F, Fu Y. Sensitivity enhancement of far-detuned RF field sensing based on Rydberg atoms dressed by a near-resonant RF field. *Opt Lett* (2022) 47(20):5256–9. doi:10.1364/OL.465048

3. Zhang LH, Liu ZK, Liu B, Zhang ZY, Guo GC, Ding DS, et al. Rydberg microwave-frequency-comb spectrometer. *Phys Rev Appl* (2022) 18(1):014033. doi:10.1103/PhysRevApplied.18.014033

4. Zhang WH, Ye YH, Zeng L, Dong MX, Li EZ, Peng JY, et al. Telecom-wavelength conversion in a high optical depth cold atomic system. *Opt Express* (2023) 31(5):8042–8. doi:10.1364/OE.481055

5. Ding DS, Liu ZK, Shi BS, Guo GC, Mølmer K, Adams CS. Enhanced metrology at the critical point of a many-body Rydberg atomic system. *Nat Phys* (2022) 18:1447–52. doi:10.1038/s41567-022-01777-8

6. Liu ZK, Zhang LH, Liu B, Zhang ZY, Guo GC, Ding DS, et al. Deep learning enhanced Rydberg multifrequency microwave recognition. *Nat Commun* (2022) 13(1):1997. doi:10.1038/s41467-022-29686-7

7. Jing M, Hu Y, Ma J, Zhang H, Zhang L, Xiao L, et al. Atomic superheterodyne receiver based on microwave-dressed Rydberg spectroscopy. *Nat Phys* (2020) 16(9):911–5. doi:10.1038/s41567-020-0918-5

8. Gallagher TF. *Rydberg atoms*. Cambridge: Cambridge University Press (2005).

9. Sedlacek JA, Schwettmann A, Kübler H, Löw R, Pfau T, Shaffer JP. Microwave electrometry with Rydberg atoms in a vapour cell using bright atomic resonances. *Nat Phys* (2012) 8(11):819–24. doi:10.1038/nphys2423

10. Mohapatra A, Jackson T, Adams C. Coherent optical detection of highly excited Rydberg states using electromagnetically induced transparency. *Phys Rev Lett* (2007) 98(11):113003. doi:10.1103/physrevlett.98.113003

11. Ryabtsev I, Beterov I, Tretyakov D, Entin V, Yakshina E. Doppler-and recoil-free laser excitation of Rydberg states via three-photon transitions. *Phys Rev A* (2011) 84(5):053409. doi:10.1103/PhysRevA.84.053409

12. He J, Liu Q, Yang Z, Niu Q, Ban X, Wang J. Noise spectroscopy with a Rydberg ensemble in a hot atomic vapor cell. *Phys Rev A* (2021) 104(6):063120. doi:10.1103/PhysRevA.104.063120

13. Xiao Y, Wang T, Baryakhtar M, Van Camp M, Crescimanno M, Hohensee M, et al. Electromagnetically induced transparency with noisy lasers. *Phys Rev A* (2009) 80(4):041805. doi:10.1103/PhysRevA.80.041805

14. Urvoy A, Carr C, Ritter R, Adams C, Weatherill K, Löw R. Optical coherences and wavelength mismatch in ladder systems. *J Phys B: Mol Opt Phys* (2013) 46(24):245001. doi:10.1088/0953-4075/46/24/245001

15. Zhou F, Jia FD, Mei J, Liu XB, Zhang HY, Yu YH, et al. The effect of the Doppler mismatch in microwave electrometry using Rydberg electromagnetically induced transparency and Autler–Townes splitting. *J Phys B: Mol Opt Phys* (2022) 55(7):075501. doi:10.1088/1361-6455/ac5d8d

16. Lahad O, Finkelstein R, Davidson O, Michel O, Poem E, Firstenberg O. Recovering the homogeneous absorption of inhomogeneous media. *Phys Rev Lett* (2019) 123(17):173203. doi:10.1103/PhysRevLett.123.173203

17. Cohen-Tannoudji C, Hoffbeck F, Reynaud S. Compensating Doppler broadening with light-shifts. *Opt Commun* (1978) 27(1):71–5. doi:10.1016/0030-4018(78)90176-1

18. Reynaud S, Himbert M, Dalibard J, Dupont-Roc J, Cohen-Tannoudji C. Compensation of Doppler braodening by light shifts in two photon absorption. *Opt Commun* (1982) 42(1):39–44. doi:10.1016/0030-4018(82)90086-4

19. Booth DW, Isaacs J, Saffman M. Reducing the sensitivity of Rydberg atoms to dc electric fields using two-frequency ac field dressing. *Phys Rev A* (2018) 97(1):012515. doi:10.1103/physreva.97.012515

20. Vogt T, Viteau M, Zhao J, Chotia A, Comparat D, Pillet P. Dipole blockade at Förster resonances in high resolution laser excitation of Rydberg states of cesium atoms. *Phys Rev Lett* (2006) 97(8):083003. doi:10.1103/PhysRevLett.97.083003

21. Bohlouli-Zanjani P, Petrus J, Martin J. Enhancement of Rydberg atom interactions using ac Stark shifts. *Phys Rev Lett* (2007) 98(20):203005. doi:10.1103/PhysRevLett.98.203005

22. Reinhard A, Younge K, Liebisch TC, Knuffman B, Berman P, Raithel G. Double-resonance spectroscopy of interacting Rydberg-atom systems. *Phys Rev Lett* (2008) 100(23):233201. doi:10.1103/PhysRevLett.100.233201

23. Hyafil P, Mozley J, Perrin A, Tailleur J, Nogues G, Brune M, et al. Coherence-preserving trap architecture for long-term control of giant Ryberg atoms. *Phys Rev Lett* (2004) 93(10):103001. doi:10.1103/PhysRevLett.93.103001

24. Mozley J, Hyafil P, Nogues G, Brune M, Raimond JM, Haroche S. Trapping and coherent manipulation of a Rydberg atom on a microfabricated device: a proposal. *Eur Phys J D-Atomic, Mol Opt Plasma Phys* (2005) 35(1):43–57. doi:10.1140/epjd/e2005-00184-7

25. Jones L, Carter J, Martin J. Rydberg atoms with a reduced sensitivity to dc and low-frequency electric fields. *Phys Rev A* (2013) 87(2):023423. doi:10.1103/PhysRevA.87.023423

26. Ni Y, Xu P, Martin J. Reduction of the dc-electric-field sensitivity of circular Rydberg states using nonresonant dressing fields. *Phys Rev A* (2015) 92(6):063418. doi:10.1103/PhysRevA.92.063418

27. Sedlacek JA, Schwettmann A, Kubler H, Shaffer JP. Atom-based vector microwave electrometry using rubidium Rydberg atoms in a vapor cell. *Phys Rev Lett* (2013) 111(6):063001. doi:10.1103/PhysRevLett.111.063001

28. Du Y, Cong N, Wei X, Zhang X, Luo W, He J, et al. Realization of multiband communications using different Rydberg final states. *AIP Adv* (2022) 12(6):065118. doi:10.1063/5.0095780

29. Meyer DH, Castillo ZA, Cox KC, Kunz PD. Assessment of Rydberg atoms for wideband electric field sensing. *J Phys B: Mol Opt Phys* (2020) 53(3):034001. doi:10.1088/1361-6455/ab6051

30. Pucher S, Schneeweiss P, Rauschenbeutel A, Dareau A. Lifetime measurement of the cesium 5D5/2 state. *Phys Rev A* (2020) 101(4):042510. doi:10.1103/PhysRevA.101.042510

31. Ray T, Gupta RK, Gokhroo V, Everett JL, Nieddu T, Rajasree KS, et al. Observation of the 87Rb 5S1/2 to 4D3/2 electric quadrupole transition at 516.6 nm mediated via an optical nanofibre. *New J Phys* (2020) 22(6):062001. doi:10.1088/1367-2630/ab8265

32. Beterov I, Ryabtsev I, Tretyakov D, Entin V. Quasiclassical calculations of blackbody-radiation-induced depopulation rates and effective lifetimes of Rydberg n S, n P, and n D alkali-metal atoms with n ≤ 80. *Phys Rev A* (2009) 79(5):052504. doi:10.1103/PhysRevA.79.052504

33. Bason MG, Tanasittikosol M, Sargsyan A, Mohapatra AK, Sarkisyan D, Potvliege RM, et al. Enhanced electric field sensitivity of rf-dressed Rydberg dark states. *New J Phys* (2010) 12(6):065015. doi:10.1088/1367-2630/12/6/065015

34. Jia FD, Liu XB, Mei J, Yu YH, Zhang HY, Lin ZQ, et al. Span shift and extension of quantum microwave electrometry with Rydberg atoms dressed by an auxiliary microwave field. *Phys Rev A* (2021) 103(6):063113. doi:10.1103/PhysRevA.103.063113